

## Vertical and Horizontal Vibration of Granular Materials: Coulomb Friction and a Novel Switching State

Sarath G. K. Tennakoon and R. P. Behringer

*Department of Physics and Center for Nonlinear and Complex Systems, Duke University, Durham, North Carolina 27708-0305*

(Received 5 February 1998)

Experiments for simultaneous horizontal ( $h$ ) and vertical ( $v$ ) vibration of granular materials show novel flow dynamics. We focus on moderate dimensionless accelerations  $0 < \Gamma_{h,v} < 1.6$ . Phenomena include the spontaneous formation of a static heap at  $\Gamma_{hs}(\Gamma_v)$  when  $\Gamma_v < 1$ , convective flow for  $\Gamma_{hc} > \Gamma_{hs}$ , and a novel switching state for frequencies  $\omega_v \neq \omega_h$ . A simple friction model provides an approximate, but not exact, description of the steady states and the transition to convection. [S0031-9007(98)06699-X]

PACS numbers: 46.10.+z, 47.20.-k, 83.70.Fn

Although granular materials are ubiquitous, their dynamical behavior is still an open problem. Consequently, granular materials have attracted considerable recent interest [1]. Granular materials can exhibit both fluidlike and solidlike properties: they resist shear up to a point, but flow under strong enough shear or at low enough density, as modeled by Coulomb friction. Important issues involve the applicability of friction-based models and the character of the dynamics when slipping occurs [2,3].

The transition between solidlike and fluidlike states is evident in shaken granular materials as seen in purely vertical vibration or purely horizontal vibration [4,5]. In these cases, a container of granular material subject to oscillations with either vertical or horizontal displacements  $s_i = A_i \sin(\omega_i t)$  has a control parameter  $\Gamma_i = A_i \omega_i^2 / g$ , where  $g$  is the acceleration of gravity, and  $i = v, h$  is for vertical and horizontal. To our knowledge, the present study is the first experimental exploration of the dynamics of granular beds subject to simultaneous horizontal and vertical vibration. We focus on two particularly interesting cases described below.

The apparatus consisted of Plexiglas cells with horizontal cross-sectional sizes ranging from 0.5 to 2.0 cm (direction perpendicular to shaking) by 12 cm (along the horizontal shaking direction). The typical cell height was 15 cm. The cell was placed on a carefully leveled shaker that provided independent vertical and horizontal displacements of the form  $s_i = A_i \sin \omega_i t$  for  $3 \leq \omega_i / 2\pi \leq 15$  Hz and  $0 < A_i \leq 20$  mm.

Typically, we varied  $A_v$  and  $A_h$  and observed the evolution of the system while keeping  $\omega_v$  and  $\omega_h$  fixed. In the first set of experiments, we vibrated the system at the same horizontal and vertical frequency with a fixed phase difference,  $\Phi = 0$ , between  $s_h(t)$  and  $s_v(t)$ . In the second set of experiments,  $\omega_h$  and  $\omega_v$  differed slightly, so that  $\Phi$  varied in time.

We used several materials, including roughly monodisperse spherical glass beads, smooth nearly spherical Ottawa sand, and sieved rough sand. These had diameters ranging from  $0.2 \leq d \leq 1.0$  mm. The layer depths were

roughly 60 mm. We prepared the system either by pouring in the selected material from a height of  $\sim 100$  mm, gently leveling the sample, and then compacting it at modest  $\Gamma_v$ , or by creating a heap at the angle of repose in the absence of shaking. The material did not form a perfectly ordered packing because the particles were not highly spherical and/or monodisperse. The results did not depend significantly on layer heights or container sizes, so long as there were enough grains to form the heap, and the container width was  $\geq 10d$ .

We characterized the flows using a strobe light, high-speed video (250 frames/s), and conventional video. Much of the data discussed here was obtained by observing the flow with a small surveillance video camera mounted on the shaker platform. To obtain the flow speeds at various locations and overall flow fields, we seeded the granular material with darker tracer particles and followed them over time.

To provide a background we first consider phenomenology for purely vertical or purely horizontal shaking. Purely vertical shaking: When  $\Gamma_v < \Gamma_{vc} \approx 1$ , the steady state is a flat layer. When  $\Gamma_v > \Gamma_{vc}$ , convective flow occurs, almost always with a single heap, and with circulatory flow of grains from the bottom to the top of the heap, then down the surface of the incline. Driving mechanisms for the flow include sidewall friction and gas effects if the grain size is  $d \leq 1$  mm. It is the gas effect that provides the main driving mechanism for the heap formation. Purely horizontal shaking: When  $\Gamma_h > \Gamma_{h*}$ , grains near the top surface of a flat layer dilate and begin to flow, while the remainder of the layer moves with the shaker in solid body motion [4,5]. This initial transition to flow is hysteretic; i.e., if flow is initiated at  $\Gamma^*$  the flow will persist to  $\Gamma < \Gamma^*$ . In addition to sloshing of the liquefied portion of the layer along the direction of shaking, two large convective rolls appear in the direction transverse to the shaking [5].

For combined vertical and horizontal sinusoidal shaking, the control parameters include  $\Gamma_v$  and  $\Gamma_h$ , and the phase difference  $\Phi$  between the two motions. We refer to

$\Phi = 0$  as “in phase” if the maximum (most positive) vertical acceleration ( $y$  direction) occurs at the same time as the maximum (most “rightward”) horizontal acceleration ( $x$  direction). The possible dynamics become much more complicated than for pure-mode shaking, and we will focus on two cases: (1) in-phase shaking when  $\Gamma_v < \Gamma_{vc}$ ; and (2)  $|f_h - f_v| \equiv \Delta f \neq 0$  but small ( $f = \omega/2\pi$ ), with  $\Gamma_v$  moderate, but not necessarily  $\Gamma < \Gamma_{vc}$ . In case (2),  $\Phi$  shifts steadily in time at the rate  $2\pi\Delta f$ .

*Case (1):*  $f_v = f_h = f_0 = \text{const}$ ;  $\Phi = 0$ ;  $\Gamma_v < \Gamma_{vc}$ .—As  $\Gamma_h$  is increased at fixed  $\Gamma_v$  with an initially flat surface, a new state forms consisting of a static heap against the “right” wall, beginning at  $\Gamma_h = \Gamma_{hs}$ . The open circles in Fig. 1 show  $\tan\theta$ , where  $\theta$  is the angle of the heap relative to horizontal versus  $\Gamma_h$  for  $\Gamma_v = 0.68$ ; the initial state was a flat surface, and  $\Gamma_h$  was gradually increased from 0. For  $\Gamma_{hs} = 0.39 < \Gamma_h < 0.6 = \Gamma_{hc}$ ,  $\theta \neq 0$  is the result of a transient, and in the steady state there is no flow until  $\Gamma_h$  exceeds a second threshold,  $\Gamma_{hc}$ . Just above  $\Gamma_{hs}(\Gamma_v)$ , a small number of surface grains

shift towards the side wall. At each value of  $\Gamma_h < \Gamma_{hc}$ , the surface motion stops when the increased slope is high enough. If instead of a flat surface, the initial state is a heap at the static repose angle against the “left” side of the container, then we find the data shown by solid squares in Fig. 1. The repose angle decreases with increasing  $\Gamma_h$ , and merges with the data obtained from an initially flat surface at  $\Gamma_{hs}$ .

This process changes when  $\Gamma_h$  exceeds a critical value  $\Gamma_{hc}(\Gamma_v)$ . At  $\Gamma_{hc}$ , the top layer along the slope liquefies and oscillates under the shaking. Any further increase in  $\Gamma_h$  increases the thickness of the liquefied layer, and decreases the average slope.

A simple Coulomb friction model [6] can capture many of the features observed in these experiments and provide additional insights (see also recent work on friction models [3]). An optimum model should predict that the instability to flow first occurs at the surface; here, we take this as a “given.” Good fits to the data based on the model can be obtained for any given property such as  $\Gamma_{hs}$  or  $\Gamma_{hc}$ , but it is not possible to accurately describe all quantities with a single set of model parameters.

We pose the model in the Fig. 1 inset. A block (a model for a surface grain) of static friction coefficient  $\mu$  is placed on a surface inclined at an angle  $\theta$ ; the surface is subject to constant vertical and horizontal accelerations,  $\Gamma_v$  and  $\Gamma_h$ , having the same sign, i.e., both positive or both negative. Negative accelerations have a vertical component in the direction of gravity. We then ask at what accelerations static friction fails.

The simplest case is a horizontal surface,  $\theta = 0$ . The block begins to slide when  $mg\Gamma_h = \mu F_n = F_t$  (where  $F_n$  and  $F_t$ —provided by friction—are, respectively, normal and tangential forces) or when  $\Gamma_h = \mu(1 - \Gamma_v) \equiv \mu(\Gamma_{vc} - \Gamma_v)$ , and the accelerations are negative. In principle,  $\Gamma_{vc} \equiv 1$ , but the data indicate that slightly higher values are needed. Henceforth, we identify  $\mu$  and  $\Gamma_{vc}$  as the two adjustable parameters of the model and the onset of sliding on a horizontal surface with  $\Gamma_{hs}$ . We examine the  $\theta = 0$  case in Fig. 2 which shows data for  $\Gamma_{hs}$  versus  $\Gamma_v$ . Except for  $\Gamma_v \approx 0$ , the data have a nearly linear profile, whose slope defines  $\mu$  and whose  $\Gamma_v$  intercept is close to 1. This intercept corresponds to the onset of heaping under purely vertical shaking, which is typically found experimentally to be somewhat larger than 1. If we force this intercept to be 1.00, the corresponding  $\mu = 1.05$ . A fit to a straight line yields  $\mu = 0.87$  and  $\Gamma_{vc} = 1.07$ . Alternatively, choosing  $\Gamma_{vc} = 1.15$  to be consistent with vertical shaking experiments leads to  $\mu = 0.80$  (dotted line).

These data also explain the extreme sensitivity in vertical shaking experiments to imperfections [7]. For  $\Gamma_v \rightarrow \Gamma_{vc}$  for vertical shaking, the system becomes unstable, and at  $\Gamma_{vc}$ , any horizontal acceleration, no matter how small, leads to slipping. Vertically shaken systems should be

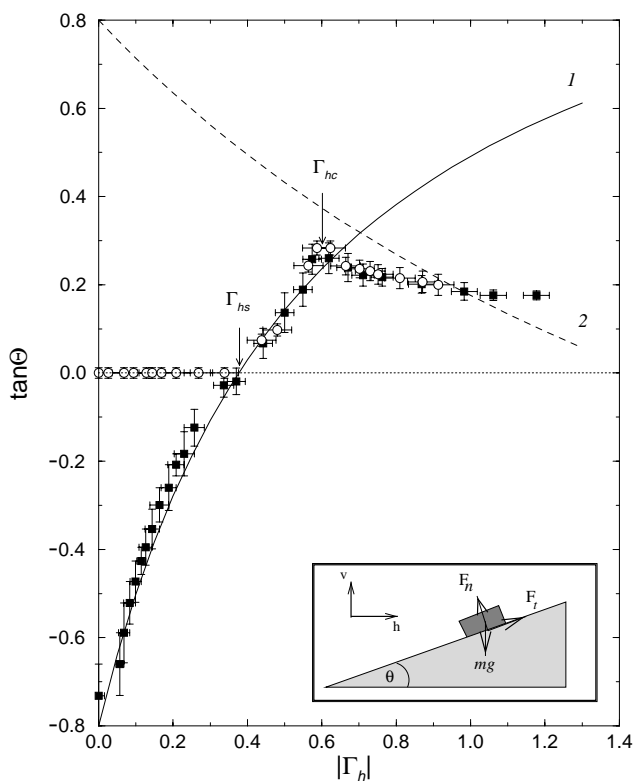


FIG. 1. Inset: sketch of inclined surface that defines the model. Open circles: heap angle,  $\theta$  of a thick (58 mm) Ottawa sand bed as a function of  $\Gamma_h$ , for  $\Gamma_v = 0.68$  for in-phase ( $\Phi = 0$ ) horizontal and vertical forcing ( $f_h = f_v = f = 4.99$  Hz,  $A_v = 6.77$  mm,  $A_h$  varying), starting from a flat surface. Solid squares: same control parameters, but starting from a heap against the left wall at the angle of repose. Lines pertain to the model; curve 1,  $\Gamma_{h,v} < 0$ , and curve 2,  $\Gamma_{h,v} > 0$ , with  $\mu = 0.80$  and  $\Gamma_{vc} = 1.15$ . Error bars in this and other figures were obtained from  $\sim$  three repetitions of the experiment.

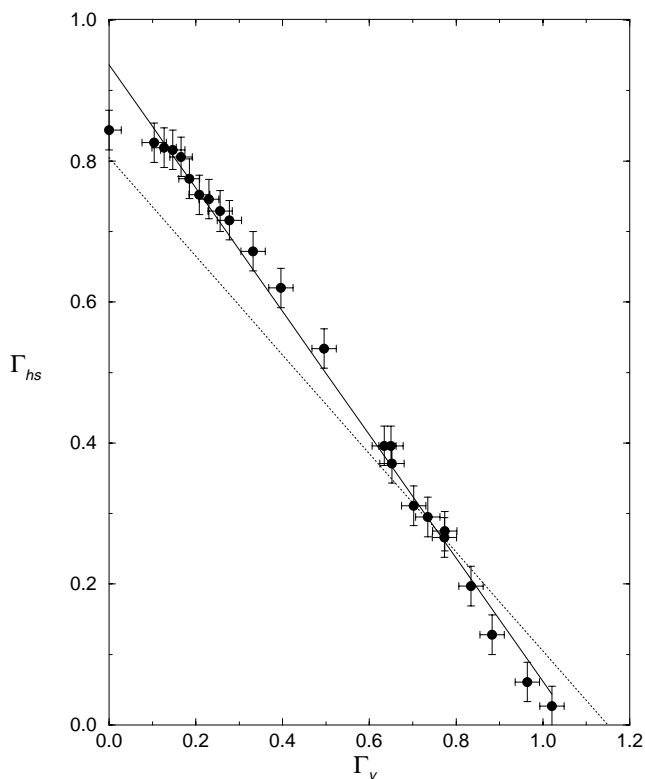


FIG. 2. Data for  $\Gamma_{hs}$  versus  $\Gamma_v$ . According to the model, these data should have a slope of  $-\mu$  and intercept at  $\Gamma_{vc} = 1$ . Solid curve: least-squares fit of the experimental data ( $\mu = 0.87$ ;  $\Gamma_{vc} = 1.07$ ); dotted curve: model with  $\mu = 0.80$  and  $\Gamma_{vc} = 1.15$ .

(and are) highly sensitive to noise in the form of small horizontal accelerations.

We next turn to the case where  $\theta \neq 0$ . We show in Fig. 1 the loci of frictional failure (or first occurrence of slipping) versus  $|\Gamma_h|$  for a fixed  $|\Gamma_v| \neq 0$ ; curve 1 (solid) is for negative  $\Gamma_h$  and  $\Gamma_v$  and curve 2 (dashed) is for positive. Curve 1 is given by  $\tan \theta = (\Gamma_h - \Gamma_{hs}) / (1 - \Gamma_v + \mu \Gamma_h)$ , and curve 2 is given by  $\tan \theta = -[\Gamma_h - \mu(1 + \Gamma_v)] / (1 + \Gamma_v + \mu \Gamma_h)$ , where we use  $\Gamma_{hs} = \mu(\Gamma_{vc} - \Gamma_v)$ . In an actual experiment, the instantaneous path is a curve, and the failure locus a surface, in a 3D space of  $\Gamma_h$ ,  $\Gamma_v$ , and  $\tan \theta$ .

We proceed with a further interpretation of this model. Stable surfaces inclined at  $\theta > 0$  persist up to the intersection of curves 1 and 2, which we identify with  $\Gamma_{hc}$ , i.e., the onset of surface flow. When a surface is prepared at  $\theta = 0$  and  $\Gamma_h$  is increased past  $\Gamma_{hs}$ , grains should flow transiently until stability is again achieved. Thus, curve 1 between  $\Gamma_{hs}$  and  $\Gamma_{hc}$  defines the slope of the static heap above  $\Gamma_{hs}$ . For  $\Gamma_h < \Gamma_{hc}$ , the heap is stable for angles lying both below curve 2 and above curve 1. Figure 1 shows  $\tan \theta$  versus  $\Gamma_h$  for Ottawa sand and  $\Gamma_v = 0.68$ . These parameters yield good agreement with the data for curve 1, but not for  $\Gamma_{hc}$ . We have also attempted to obtain experimental data for curve 2, but this

proved difficult because of initial transients. In Figs. 3(a) and 3(b) we consider  $\Gamma_{hc}$  and  $\tan \theta$  at  $\Gamma_{hc}$ , respectively, versus  $\Gamma_v$ . The solid curves in each part of this figure correspond to  $\mu = 0.80$  and  $\Gamma_{vc} = 1.15$ . The agreement with this common set of parameters is not very good. For each of these quantities, good fits can be obtained (dot-dashed curves) but the necessary coefficients, given in the caption, are not mutually consistent.

*Case (2):  $\omega_h \neq \omega_v$ .*—Before closing, we explore a related and novel phenomenon which occurs when the shaking frequencies differ by a small amount so that  $\Phi$  varies in time. We begin by considering the case of fixed nonzero phases. For  $\Phi = 0^\circ$  or  $\Phi = 180^\circ$ , the heap forms next to one or the other of the vertical sidewalls. When  $\Phi$  is close to  $90^\circ$ , the heap height is reduced and is located near the middle of the cell. When the frequencies of vertical and horizontal shaking are slightly different,  $\Phi$  changes periodically with frequency  $\Delta f$ , causing the heap to move from one wall to the other and reversing the convective flow field. Figure 4 shows the surface of the heap for various times as the heap switches from one side to the other. Here  $\Gamma_v > 1$ , but the case  $\Gamma_v < \Gamma_{vc}$  is similar. From the discussion above, the heap forms along whichever wall is pushing on the

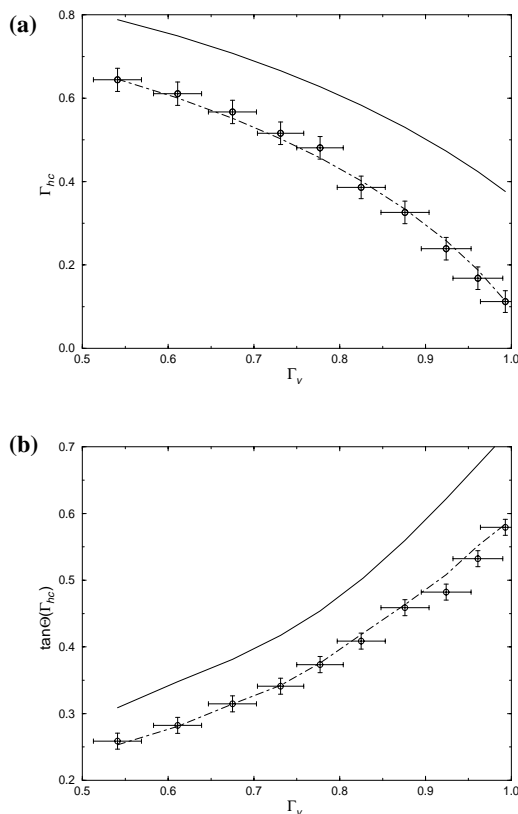


FIG. 3. Points: data for (a)  $\Gamma_{hc}$ , and (b)  $\tan \theta$  at  $\Gamma_{hc}$  versus  $\Gamma_v$ . Solid curves show predictions of the Coulomb friction model for  $\mu = 0.80$  and  $\Gamma_{vc} = 1.15$ . Dot-dashed curve in (a) is for  $\mu = 0.77$  and  $\Gamma_{vc} = 1.03$  and in (b) is for  $\mu = 0.65$  and  $\Gamma_{vc} = 1.35$ .

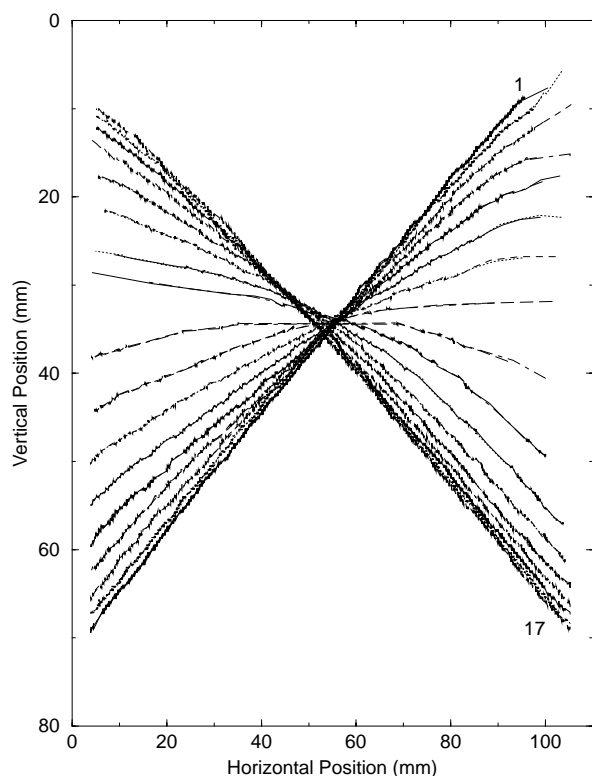


FIG. 4. Shape of the top surface at various times during a switch from one side to the other. The time between the curves is 2 s and the period of back and forth heap motion is 180 s. (Here we show the shape of the top surface for 34 s; for the following 46 s the heap remains on the left wall with nearly the same shape as curve 17.)

material during the negative vertical acceleration portion of the cycle. The heap remains near that wall until the horizontal acceleration switches direction relative to the vertical acceleration.

In conclusion, we have characterized flows that appear in a granular bed subject to both horizontal and vertical vibrations. Properties such as static heaping and convection depend on  $\Gamma_v$ ,  $\Gamma_h$ , and the phase difference  $\Phi$ . The static heap formation and the onset of flow are captured semi-quantitatively by a Coulomb-type friction model. However, these experiments point to the need for an improved

picture, possibly including the effects of fabric or other history-dependent features, since it is necessary to adjust the relevant parameters in order to describe different aspects of the flow. We emphasize that the transitions to flow described here are not likely to depend fundamentally on the presence of air, unlike the heaping instability for vertically shaken small-grained materials.

We appreciate helpful comments by Dr. Stéphane Roux, and by Professor David Schaeffer and Professor Joshua Socolar. This work was supported by NASA under Grant No. NAG3-1917 and by NSF Grants No. DMR-9321791 and No. DMS-9504577.

- 
- [1] H. M. Jaeger, S. R. Nagel, and R. P. Behringer, *Rev. Mod. Phys.* **68**, 1259 (1996); *Phys. Today* **49**, No. 4, 32 (1996). See also R. P. Behringer, *Nonlinear Sci. Today* **3**, 1 (1993); *Granular Matter: An Interdisciplinary Approach*, edited by A. Mehta (Springer-Verlag, New York, 1994); H. M. Jaeger and S. R. Nagel, *Science* **255**, 1523 (1992); D. Bideau and J. Dodds, in *Physics of Granular Media*, Les Houches Series (Nova Science Publishers, Commack, NY, 1991).
  - [2] S. Nasuno, A. Kudrolli, and J. P. Gollub, *Phys. Rev. Lett.* **79**, 949 (1997).
  - [3] J. P. Wittmer, P. Claudin, M. E. Cates, and J.-P. Bouchaud, *Nature (London)* **382**, 336 (1996); for a review of older models, see R. Jackson, in *The Theory of Dispersed Multiphase Flow*, edited by R. Meyer (Academic Press, New York, 1983).
  - [4] P. Evesque, *Contemp. Phys.* **33**, 245 (1992); J. A. C. Gallas, H. J. Herrmann, and S. Sokolowski, *J. Phys. II (France)* **2**, 1389 (1992); G. H. Ristow, G. Strassburger, and I. Rehberg, *Phys. Rev. Lett.* **79**, 833 (1997); O. Pouliquen, M. Nicolas, and P. D. Weidman, *Phys. Rev. Lett.* **79**, 3640 (1997); K. Liffman, G. Metcalfe, and P. Cleary, *Phys. Rev. Lett.* **79**, 4574 (1997).
  - [5] S. G. K. Tennakoon, L. Kondic, and R. P. Behringer (to be published).
  - [6] M. E. Vavrek and G. W. Baxter, *Phys. Rev. E* **50**, R3353 (1994).
  - [7] E. Clément, J. Duran, and J. Rajchenbach, *Phys. Rev. Lett.* **69**, 1189 (1992); C. E. Beaseley, E. van Doorn, and R. P. Behringer (to be published).